

# Airborne SAR Tomographic Ice Sheet Sounding

Xiaoqing Wu, Jet Propulsion Laboratory, USA  
Ken Jezek, Ohio State University, USA  
Ernesto Rodriguez, Jet Propulsion Laboratory, USA  
Prasad Gogineni, University of Kansas, USA  
Anthony Freeman, Jet Propulsion Laboratory, USA

## Abstract

A new tomographic ice sounding method is introduced to provide airborne swath measurements of ice sheet thickness and basal scattering properties. Two major challenges have been solved: left-right signal separation; and surface clutter rejection. The new technique was demonstrated using data we collected in 2006 and 2008 from a VHF-band, multiple phase-center radar system flown in Greenland. For the first time we were able to “see” radar images of the base of the ice sheet.

## 1 Introduction

Glaciers and ice sheets modulate global sea level by storing water deposited as snow on the surface and discharging water back into the ocean through melting. Their physical state can be characterized in terms of their mass balance and dynamics [1]. To have knowledge of the current ice mass balance and to predict ice sheet dynamics in Greenland and Antarctica, we need to know the ice sheet thickness and the physical properties of the ice sheet surface and bed. We require this information at fine resolution and over extensive portions of the ice sheets.

Conventional ice sounding provides one dimensional thickness measurements of the ice sheets along the flight lines of the radar sounder [2, 3]. Here, the along track resolution is met by forming a synthetic aperture, nadir signals are enhanced by using an antenna array, and the vertical resolution of the thickness is met by transmitting a high bandwidth signal. Even though highly accurate thickness measurements can be achieved [4], information in the third cross track dimension is at best suppressed.

Microwave synthetic aperture radar (SAR) [5] and SAR interferometry [6] have been widely used for swath 2-D and 3-D terrestrial and ice sheet [7] surface mapping. These airborne and space-borne measurements all used the side-looking configuration. Ice sounding radars all use very low frequencies ranging from 1 MHz to 500 MHz in order for the signal to penetrate the ice mass.. For such a low frequency the back scattering from the ice surface and the bottom decreases quickly as the incidence angle increases. At these low frequencies it is difficult to design an antenna array with sufficient side-lobe suppression to implement a side-looking SAR with wide swath. Consequently, we sought a signal processing solution to

this problem by adopting tomographic approaches developed in other fields.

The term tomography originated from computer aided tomography imaging [8]. It was first applied to spotlight SAR processing in 1983 for azimuth compression [9]. By 2000, SAR tomography began to appear in the literature [10], where the authors used 14 repeat passes to estimate the 3-D topography of forests, buildings and terrains. We adapted SAR tomography for the purpose of ice sheet sounding as discussed below. We applied the procedure outlined in section II to data we collected in May 2006 and September 2008 using 150 MHz multiple channel ice sounding radar developed at the University of Kansas, USA.

## 2 Two Dimensional Ice-Sounding

In this section we formulate 2-D ice-sounding as a problem of estimating signal arrival angles. The ice mass has two major interfaces, the upper surface interface, between the air and the ice mass, and the basal interface, between the ice mass and bedrock or basal water. In between there are weak internal layers that originate from slight density changes or from ancient volcanic deposits. When the radar signal reaches the air-ice interface, some of the energy is scattered back and some refracts through the interface and continues travelling through the ice mass. Some of the transmitted signal will scatter back towards the receiver from the basal interface. Simultaneous with the nadir echo arriving from the bedrock the receiver may also detect the surface reflected signal from both the left and right sides of the sensor. Off nadir, there may also be simultaneous echoes from the base originating from the opposite sides of the airplane. In addition, there will be thermal and other noise sources. If the sounder altitude is low, the surface clutter from both sides arrives from large incidence angles compared

with the same range bin occupied by the bottom signal. Thus the surface clutter strength is weak and the bottom signal is strong, relatively. In this case the challenge for swath imaging is to separate returns from the left and right side of the aircraft. If the sounder altitude is high, the surface clutter arises from only somewhat larger incidence angles and so will be relatively strong compared to the basal return, which is attenuated by absorption through the ice. So we must separate left and right bottom signals, and we also must reject the surface clutter as well in order to get the desired bottom signal. Fig. 1 shows the ice-sounding geometry and the challenges we need to solve.

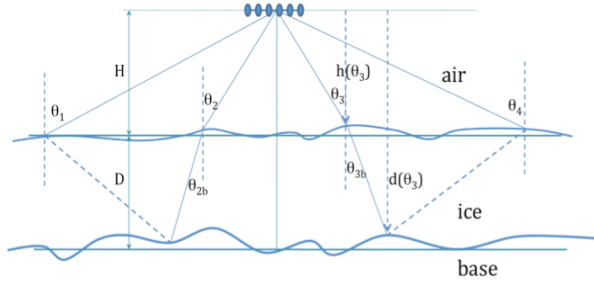


Fig. 1 Tomographic ice-sounding geometry

For each channel of our multiple channel radar, we begin by forming a SAR image. After image formation, we have one measurement for each along track image position and each slant range bin. If we consider a two-layer model as shown in Fig. 1, the measurements within each range bin include left and right surface components, and left and right basal components along with noise. Mathematically, we have

$$\begin{bmatrix} x_1 \\ x_2 \\ \vdots \\ x_p \end{bmatrix} = \begin{bmatrix} e^{jkd_1 \sin \theta_1} & e^{jkd_1 \sin \theta_2} & \dots & e^{jkd_1 \sin \theta_q} \\ e^{jkd_2 \sin \theta_1} & e^{jkd_2 \sin \theta_2} & \dots & e^{jkd_2 \sin \theta_q} \\ \vdots & \vdots & \dots & \vdots \\ e^{jkd_p \sin \theta_1} & e^{jkd_p \sin \theta_2} & \dots & e^{jkd_p \sin \theta_q} \end{bmatrix} \begin{bmatrix} s_1 \\ s_2 \\ \vdots \\ s_q \end{bmatrix} + \begin{bmatrix} n_1 \\ n_2 \\ \vdots \\ n_p \end{bmatrix} \quad (1)$$

where  $x_i$  is received signal of channel  $i$ ,  $k$  is the wave number  $4\pi/\lambda$ ,  $d_i$  is distance of channel  $i$  to the left most channel,  $\theta_j$  is the arrival angle of signal  $j$ ,  $p$  is the number of channels,  $s_i$  is the complex amplitude of signal  $j$ ,  $q$  is the number of signals and  $n_i$  is the noise received in channel  $i$ . For the case shown in Fig. 1, the number of simultaneous signals  $q$  is 4. Equation (1) can be expressed in vector and matrix form as

$$X = A(\Theta) \cdot S + N \quad (2)$$

We seek the arrival angle vector  $\Theta$  and the signal vector  $S$  using the available measurement of vector  $X$  and the known geometry of the transmit and receive antenna array. This problem is exactly the same as that of direction-of-arrival (DOA) estimation in array signal processing. Many algorithms have been proposed

to solve the problem. Among them are conventional beam forming, MUSIC [11], maximum likelihood (ML) [12, 13] and so on. For statistically independent, stationary and ergodic complex Gaussian thermal noise and uncorrelated signals, the maximum-likelihood method provides a solution, which is very close to the optimum [12, 13].

The ML solution of the arrival angle vector and the signal vector can be expressed as [14]

$$\min_{\Theta} = \text{tr}[A(\Theta)(A^H(\Theta)A(\Theta))^{-1}A^H(\Theta)R] \quad (3)$$

After the ML solution of the arrival angle and signal vectors are found, the relative surface elevation  $h$ , which is the vertical distance between the sensor horizontal plane and the air-ice interface point, and the base depth  $d$ , can be calculated from the arrival angle and the slant range.

### 3 Demonstration of left-right separation

The relative contamination of signals arriving simultaneously from the surface and bed depends on the sensor altitude. In May 2006 we collected data in northern Greenland at an altitude of about 600m above the ice surface. The data were collected over the interior ice sheet and in a region where there is little if any surface melt. After range compression and azimuth compression, we produce a complex image for each phase center channel.

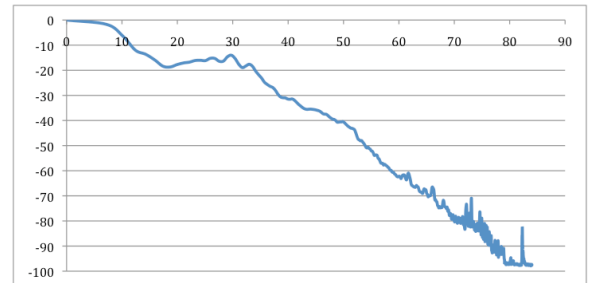


Fig. 2 Typical surface, internal layers and base scattering strength (in dB) as a function of equivalent surface incidence angle (in degrees).

The ice thickness for the scene is about 2250m, so the near-nadir basal-return arrives coincident with a surface clutter return originating at a look angle of  $82^\circ$ . The surface return will be relatively weak in part because of decreasing antenna gain due to increasing look angle and in part because of the reduction of scattering coefficient with increasing incidence angle. For 150 MHz carrier frequency, Fig. 2 shows the typical surface, internal layers and the base scattering strength as a function of surface clutter incidence angle. According to Fig. 2 surface clutter and internal layer returns reached the thermal noise floor of about -98dB at about  $78^\circ$ . On the other hand, the nadir and slightly off-nadir returns from the base are much stronger than the surface clutter even though the returned base signal

has been attenuated as it travels through the ice mass (1-2dB per 100 m depending on ice temperature). The base returns start to appear at a surface equivalent incidence angle of  $82.2^\circ$  with a strength of -83dB.

Because surface and basal returns dominate at different equivalent incidence angles, we can assume only two signals contributed to the returns at any one time in equations (1). Hence, we can estimate the surface topography and intensity from the near range measurements. The far range measurements are then used to estimate the two base components assuming that the surface components are weak enough to be ignorable. In any case both the surface and the base components can be estimated by a two dimensional search of equation (3). Other faster algorithms [14] can also be used to speed up the minimization process. The data sets we collected in northern Greenland in May 2006 were used to demonstrate the technique. The multiple channel ice sounding radar system, which was developed at the University of Kansas, has two transmitting antennae and 6 receiving antenna elements. The system operated in ping-pong mode, which means the left and right transmitting antenna worked alternating. This mode gives us total 12 equivalent receiving phase centers. After range compression and azimuth compression, we got a complex image for each phase center channel. The conventional ice sounding technique is to use intensity images to measure the ice thickness of the nadir.

For each pixel in the image, 12 measurements from the 12 phase center channels are used to solve the left and right arrival angles and the left and the right signal strengths. The ice thickness can be then calculated using equation (2) and (3). Fig. 3a shows the estimated ice thickness map in azimuth and ground range geometry. The corresponding intensity map is shown in Fig. 3b.

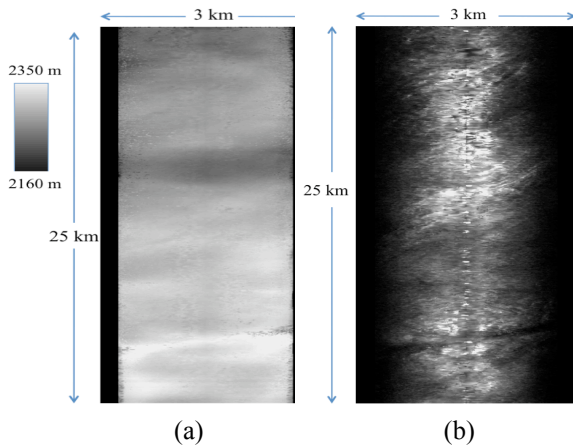


Fig. 3 estimated (a) ice thickness map and (b) bed intensity in azimuth and ground range geometry

The base topography and intensity images shown in Fig. 2 are the first ones of this kind. The airborne tomographic ice sounding technique provides both the ice thickness and the intensity measurements for the whole swath.

#### 4 Surface clutter rejection

Although two dimensional ice sounding was achieved by using the tomographic ice sounding technique described in section 3, the achieved swath width is limited because of low backscattering for large off-nadir angles. There are two ways to increase the ice sounding swath width. One way is to increase transmitting power to maintain a good SNR even for large off-nadir look angles. But the transmitting power cannot be increased without limitation and in any case, back scatter from the base decreases rapidly as the incidence angle increases. Based on our observations, it is fair to assume that for reasonable transmitting power (1-2 kW),  $20^\circ$  is about the average maximum incidence angle, beyond which the base back scattering becomes too weak compared with the thermal noise. The second solution is to increase the sensor platform altitude, which can be easily done. However, sensor altitude increase results in the increase of the surface clutter level, which now requires that the minimum number of signals considered in the tomographic processing be increased to 4. To test this approach, the same radar system with additional antenna elements was used to collect high altitude data in September 2008. The platform altitude above the ice sheet varied during the whole flight. But for the data sets we show, the average platform altitude is about 3 km.

Fig. 4a is the intensity image constructed from the incoherent sum of all the phase center channels. The base is barely seen in Fig. 4a. Fig. 4b shows the result of beam steering with 4 phase centers and Hamming window weighting. It shows clearly that beam steering is the right method for surface clutter rejection if nadir profile ice sounding is the objective.

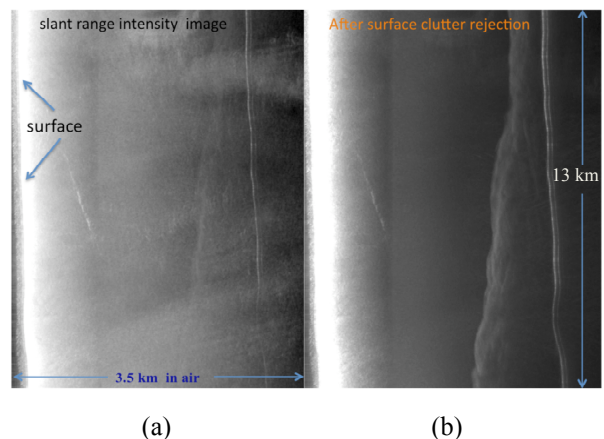


Fig. 4 intensity images before (a) and after (b) applying beam steering.

The results shown in Fig. 4 illustrate that surface returns dominate up to surface equivalent incidence angles of about  $52^\circ$ . The nadir base return arrives at slant ranges where the corresponding surface returns have an incidence angle bigger than  $52^\circ$ . Subsequently, off nadir basal returns and surface returns are mixed. Estimating surface topography and intensity can be simply done using the procedure described in section 3 and by assuming left and right surface signals only. For far range bins where both surface clutter and base signals are included, a 4 dimensional search is needed to get the ML solution of equation (4). Since a 4-dimensional search is computationally expensive, we used a suboptimal approach to reduce the computational complexity to a reasonable level. This sub-optimal approach includes estimating the two surface components, removing surface components from the original measurements and then estimating the two base components from the residual data. MUSIC [11] algorithm can also be used to solve equation (4) for a suboptimum solution.

By using the procedure described above we were able to get a good estimate of the ice sheet thickness and the bottom back scattering intensity. Fig. 5 shows the ice thickness image (Fig. 5a) and the intensity image (Fig. 5b) in azimuth and ground range geometry, respectively.

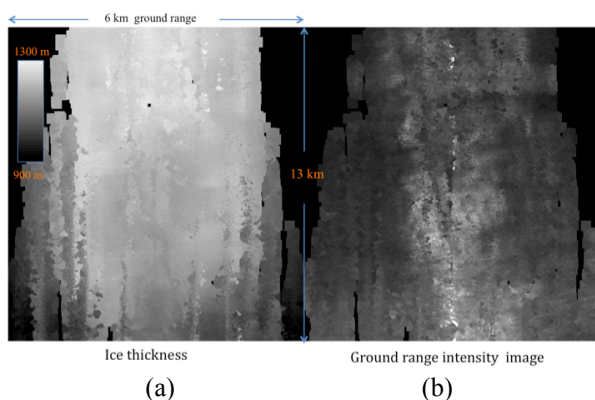


Fig. 5 ice thickness (a) and intensity (b) image in azimuth and ground estimated from high elevation data

## 5 Conclusions

We have demonstrated that airborne tomographic ice-sounding can be used for mapping the 3-d surface and base of ice sheets. For the first time we were able to measure two dimensional topography and scattering properties of the bottom of kilometer thick ice sheets.

## Acknowledgements

This work was supported by National Aeronautics and Space Administration (NASA) instrument incubator and Polar Oceans and Ice Sheets Program and the NSF CReSIS project.

## References

- [1] K. Jezek, E. Rodriguez, P. Gogineni, A. Freeman, J. Curlander, X. Wu, J. Paden, C. Allen, "Glaciers and Ice Sheets Mapping Orbiter Concept", *Journal of Geophysical Research*, Vol. 111, May 2006.
- [2] D. Blankenship, et al., "Feasibility study and design concept for an orbiting ice-penetrating radar sounder to characterize in three-dimensions the European ice mantle down to any ice/ocean interface", technical report, JPL, California, USA.
- [3] P. Gogineni, T. Chuah, C. Allen, K. Jezek, R.K. Moore, "An improved coherent radar depth sounder", *J. Glaciology*, 44(1480), 659-669, 1998.
- [4] Keith Raney, "Cross-Track Polarimetric Selectivity", EUSAR 2008.
- [5] J. Curlander, R. McDonough, "Synthetic Aperture Radar: Systems and Signal Processing", 1992.
- [6] H. Zebker, R. Goldstein, "Topographic mapping from interferometric synthetic aperture radar observations", *J. Geophys Res.*, Vol 91 (B5), pp. 4991-4999, April, 1986.
- [7] K. Jezek, R. Carande, K. Farness, X. Wu, J. Miller, "RADARSAT observations of Antarctica from Modified Antarctic Mapping Mission 2000", *Radio Science*, 2003.
- [8] H.J. Scudder, "Introduction to computer aided tomography", *Proc. IEEE*, Vol. 66, pp628-637, 1978.
- [9] D. Munson, J. O'Brien, W. Jenkins, "A Tomographic Formulation of Spotlight-Mode Synthetic Aperture Radar", *Proc. IEEE*, Vol. 71, No. 8, August, 1983.
- [10] A Reggber, A. Moreora, "First demonstration of airborne SAR tomography using multibaseline L-band data", *Geoscience and Remote Sensing, IEEE Transactions*, Vol. 38, Issue 5, Sep, pp2142-2152, 2000.
- [11] R. Schmidt, "Multiple Emitter Location and Signal Parameter Estimation", *IEEE Trans. On Antenna and Propagation*, Vol. AP-34, No. 3, March, 1986.
- [12] P. Stoica, A. Nehorai, "MUSIC, maximum likelihood, and Cramer-Rao bound", *IEEE Trans. On acoustics speech and signal processing*, Vol. 37, No. 5, May 1989.
- [13] P. Stoica, A. Nehorai, "MUSIC, maximum likelihood, and Cramer-Rao bound: further results and comparisons", *IEEE Trans. On acoustics speech and signal processing*, Vol. 38, No. 12, December 1990.
- [14] I. Ziskind, M. Wax, "MUSIC, maximum likelihood localization of multiple sources by alternating projection", *IEEE Trans. On acoustics speech and signal processing*, Vol. 36, No. 10, October 1988.